Journal of the European Ceramic Society **9** (1992) 193–204

Kinetic Demixing Profile Calculation under a Temperature Gradient in Multi-component Oxides

D. Monceau, C. Petot & G. Petot Ervas*

CNRS-LIMHP, Université Paris Nord, Av. J.B. Clément 93430 Villetaneuse, France

(Received 8 April 1991; revised version received 26 July 1991; accepted 12 August 1991)

Abstract

This paper presents time-dependent cation redistribution simulations in multi-component semiconducting oxides under a temperature gradient. Such effects are an important source of material deteriorations at high temperature. This calculation has allowed the authors to show how kinetic demixing takes place and how the phenomena is related to the transport properties of the material. Both the magnitude and the time-dependent kinetic demixing have been determined for the (Co, Mg)O system for which cation diffusion coefficient values and defect concentrations are available.

In dieser Veröffentlichung werden Simulationen der zeitabhängigen Kationenumverteilung in mehrkomponentigen halbleitenden Oxiden unter dem Einfluß eines Temperaturgradienten vorgestellt. Solche Effekte sind eine entscheidende Quelle für die Verschlechterung der Materialeigenschaften bei hohen Temperaturen. Diese Berechnung ermöglicht den Autoren zu zeigen, wie die Entmischungskinetik verläuft und wie das Phänomen mit den Transporteigenschaften des Materials zusammenhängt. Beides, sowohl die Größenordnung als auch die Zeitabhängigkeit der Entmischungskinetik, wurde für das (Co, Mg)O-System, für welches Angaben über die Kationen-Diffusionskoeffizienten und die Defektkonzentrationen verfügbar sind, bestimmt.

Cet article présente des simulations concernant la redistribution cationique en fonction du temps sous l'influence d'un gradient de température, dans des oxydes semiconducteurs à plusieurs composants. De tels effets sont une source importante de détérioration des matériaux à haute température. Ce calcul a permis aux auteurs de montrer comment la démixtion cinétique se déroule et comment le phénomène est lié aux propriétés de transport du matériau. L'importance et la dépendance en temps de la démixtion cinétique ont été déterminées pour le système (Co, Mg)O, pour lequel les valeurs de coefficients de diffusion cationique et de concentrations en défauts sont disponibles.

1. Introduction

Due to their remarkable stability ceramics are most often used for high-temperature technologies such as in heat exchangers, in magnetohydrodynamic (MHD) generators (as electrode materials) or in nuclear energy, for example. In such applications, ceramics are generally exposed to important temperature changes. A temperature gradient generally leads to directed diffusion of species. These transport processes may be responsible for cation redistributions and demixing processes, which are important sources of material deterioration at high temperature. From an industrial point of view, the knowledge and the understanding of these kinetic demixing processes is one of the keys to improving the durability and reliability of engineered materials exposed to important temperature changes. Nevertheless, despite the importance of such effects, little is known for ceramics and most of the results are available for metals. This is due partly to the lack of diffusion data and partly to the difficulty of performing reliable analysis on isolating materials as ceramics, until recently.

In previous papers[1,2] the authors have analysed kinetic demixing effects near surfaces in ceramic materials under a temperature gradient or during cooling and have recalled some technological

* To whom correspondence should be addressed.

Journal of the European Ceramic Society 0955-2219/92/$5.00

consequences of these effects in ceramic powder preparation or in the ageing of ceramics subject to large temperature changes, for example. On the other hand, Petuskey & Bowen[3] have studied the conditions leading to the demixing of cations in an iron aluminate spinel when this material is exposed to a temperature gradient. They have observed that the matter transport seems to be due in the considered materials mainly to the driving force of the chemical potential gradient, which appears simultaneously to the thermal driving force when exchange with the surrounding atmosphere is possible. Akbar *et al.*[4] have investigated, by the path probability method of irreversible statistical mechanics, the demixing of oxide solid solutions under a temperature gradient. Their calculations have been performed under two different conditions: (i) at a steady state (no flow of matter with respect to the crystal reference frame while it moves with a constant velocity with respect to the laboratory reference frame), and (ii) in a closed system (Soret effect). In this last case, the surfaces of the system are blocked from the oxygen atmosphere and their results confirm those of Petuskey & Bowen,[3] who observed a negligible redistribution of cations when exchange with the surrounding atmosphere is not possible.

On the other hand, kinetic demixing studies in ceramics under a chemical potential gradient at constant temperature have been the subject of different papers in the last decade.[5-12] Some experimental results have shown the influence of an oxygen potential gradient on the degradation of materials such as (Co, Mg)O,[6-8] Ni_2SiO_4,[11] Fe_2SiO_4[6] or $NiTiO_3$,[6] for example. Calculations have been done by Schmalzried and coworkers[6-8] at the steady state, i.e. when the cationic species in the material move with the same velocity, equal to the shift velocity of the crystal with respect to the laboratory reference frame. It can be pointed out that this state can be reached only after a long time and when no precipitation of new phases appears during the transport processes such as in the solid solutions (Co, Mg)O studied by Schmalzried and coworkers.[6-8] As an example, cation redistributions after an annealing time of 136 h are reported in Fig. 1 as well as the segregation profile calculated by Schmalzried and coworkers for the steady state. Ishikawa *et al.*[12] tried to follow the transient period, but their calculations in the general case were stopped by a problem of numerical instability. Recently, the present authors were able to follow[9,10] the time evolution of the kinetic demixing profile in multi-component compounds from the change of the thermodynamical equilibrium conditions until the steady state was reached. The calculation was done using a numerical model and was applied to the (Co, Mg)O system. A good agreement was observed between these calculated values and the experimental results of Schmalzried and coworkers,[6-8] which confirms the assumption of the formal treatment (Fig. 1). Furthermore, this calculation has allowed the estimation of the time needed to reach a steady state.[10] This time has been found higher than 300 h for (Co, Mg)O solid solutions at 1439°C (Fig. 1).

The main aim of this paper is to provide a calculation method for time evolution of kinetic demixing profiles in ceramics under a temperature gradient and to try to show the conditions leading to cation redistributions. This analysis has been done taking into account the recent experimental results of thermomigration of Petuskey & Bowen.[3] Time-dependent cation redistributions have been estimated for the system (Co, Mg)O for which diffusion data and defect concentrations are available and

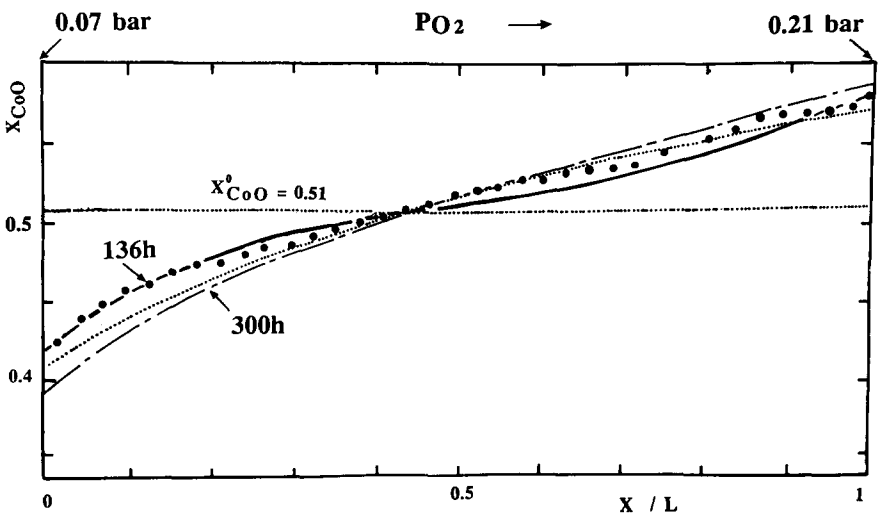

Fig. 1. Experimental kinetic demixing profiles in (Co, Mg)O solid solutions annealed for 136 h at 1712 K under an oxygen potential gradient between 0·07 and 0·21 bar. Sample length $L = 600\,\mu m$. Comparison of the experimental (●) and calculated (steady state) (···) results of Schmalzried and coworkers[6-8] and calculated results of Monceau *et al.*[10] after 136 h (——) and 300 h (— - — - —).

which can be considered as a model material. Nevertheless, the formalism used can be applied to all semiconducting ceramics (A, B)O in which the prevailing defects are present on the cationic sublattice (vacancies or interstitials) and which form an important class of ceramic materials.

2 Statement of the Problem

2.1 General approach

Consider a multi-component oxide, such as the solid solutions (Co, Mg)O. In these materials oxygen ions are practically immobile and form a rigid lattice, while vacancies exist in the cationic sublattice and are responsible for the matter transport. It is assumed that at high temperatures the end surfaces of the oxide are always in equilibrium with the surrounding atmosphere. The concentration of vacancies on these surfaces is then controlled by the thermodynamical equilibrium conditions (T and P_{O_2}). For an oxide AO_γ, their formation can be described by the following equation:

$$\gamma/2O_2 \leftrightarrows V_A^{\alpha'} + \alpha h^{\cdot} + \gamma O_o \qquad (1)$$

from which it follows, according to the mass action law and to the electroneutrality condition ($\alpha[V_A^{\alpha'}] = [h^{\cdot}]$):

$$[V_A^{\alpha'}] = \alpha^{-\alpha/1+\alpha} K^{1/1+\alpha} P_{O_2}^{\gamma/2(1+\alpha)} \qquad (2)$$

where O_o, $V_A^{\alpha'}$ and $h^{\cdot}$ denote a neutral anion on an anion site, an α-times ionized cation vacancy and an electron hole, respectively. γ is related to the charge state of the cations (in the case of a divalent cation A^{2+}, $\gamma = 1$). The square brackets denote the concentration of defects per mole of AO_γ, K is the equilibrium constant related to the standard free enthalpy of formation of the defects (ΔG_f) by the following equation:

$$-RT\ln K = \Delta G_f = \Delta H_f - T\Delta S_f \qquad (3)$$

After a change of temperature at constant oxygen partial pressure, it follows from eqns (2) and (3) that the concentration of vacancies can increase or decrease[13] according to the sign of the enthalpy of formation of the defects (ΔH_f).

In a general way, after an abrupt change of the thermodynamical equilibrium conditions (T or P_{O_2}) the sample reacts with the surrounding atmosphere according to eqn (1). This leads to an irreversible flow of vacancies through the end surfaces accompanied by a flow of cations in the sample and by the creation or annihilation of lattice sites on the end surfaces. Therefore, a concentration gradient of cations would develop if the jump frequencies between the vacancies and the cations A and B are different. In previous papers[9,10] the authors have analysed the kinetic demixing processes under a chemical potential gradient, at constant temperature. It has been shown[9,10] that the diffusion of cations under an oxygen potential gradient can be treated as diffusion under the concentration gradient of cationic vacancies. Indeed, after an abrupt change of P_{O_2}, the local chemical equilibrium near the surfaces (eqn (1)) is expected to set up rapidly. This leads to a vacancy concentration gradient given by the following equation when $\gamma = 1$:

$$\delta \ln [V^{\alpha'}]/\delta x = (1+\alpha)^{-1}\, \delta \ln a_o/\delta x \qquad (4)$$

A flux of vacancies (J_V) occurs then in the material toward the side of the lower P_{O_2}. This flux is of course accompanied by a flux of cations in the opposite direction. Far from vacancy sources and sinks, lattice sites are conserved. Relative to the rigid oxygen sublattice the fluxes of cations (J_i) and vacancies are coupled through the condition:

$$J_V + \sum J_i = 0 \qquad (5)$$

2.2 Driving force of demixing under an oxygen potential gradient

In the following the main steps, which enabled the authors previously[2,9,10] to obtain a quantitative formulation of the transport processes under an oxygen potential gradient and to identify the driving force for cation diffusion as the vacancy concentration gradient, will be recalled briefly. Indeed, in iono-covalent compounds, the fluxes of the cationic species i are generally expressed as a function of the driving force of the electrochemical potential gradient ($\delta\eta_i/\delta x$) (if correlation effects are neglected, i.e. the off-diagonal elements L_{ij} in a phenomenological formulation, which corresponds to weak cation-vacancy binding energies in the considered materials):

$$J_i = -C_M(D_i/RT)[i](\delta\eta_i/\delta x)_T \qquad (6)$$

where, C_M is the overall concentration (in mol cm^{-3}) of the cationic sites and $[i]$ the mole fraction of cations A or B.

In semi-conducting materials, it can be shown that the electrochemical potential (η_i) of the cations is related to the chemical potential (μ_i) of the neutral species,[9,14] by the following equation:

$$\delta\eta_i/\delta x = \delta\mu_i/\delta x = RT\,\delta \ln a_i/\delta x \qquad (7)$$

where a_i is the thermodynamical activity of the species i.

From eqns (6) and (7), according to the electroneutrality condition and assuming a local chemical

equilibrium between the different species ($1/2O_2 + A \leftrightarrows AO$, $\gamma/2O_2 + B \leftrightarrows BO\gamma$) in each element of volume of the oxide solid solution (A, B)O, it has been shown that the flux of cations with respect to the anion sublattice (which coincides with the external laboratory reference frame) can be written as follows[9,10] (when $[V^{\alpha'}] \ll m$ and $(1-m)$):

$$J_{A^{2+}} = C_M D_A(\delta m/\delta x + (1-m)(1+\alpha)\,\delta \ln [V^{\alpha'}]/\delta x) \quad (8)$$

$$J_{B^{2+}} = C_M D_B(-\delta m/\delta x + m\gamma(1+\alpha)\,\delta \ln [V^{\alpha'}]/\delta x) \quad (9)$$

where $\delta[V^{\alpha'}]/\delta x$ is the vacancy concentration gradient at constant temperature given by eqn (4), m the mole fraction of the cations B, $\delta m/\delta x$ their concentration gradient, and D_A and D_B the diffusion coefficients of the cations A and B, respectively.

2.3 Driving forces of demixing under a temperature gradient

When an iono-covalent compound is exposed to a temperature gradient, the flux of cations which then appears in the material has been assumed previously in the literature[15,16] to be proportional to a linear combination of the driving force of the electrochemical potential gradient at constant temperature $(\nabla \eta_i)_T$ and of the thermal driving force ($\nabla \ln T$). If the correlation effects are neglected, this equation can be written in a one-dimensional form, as follows:

$$J_i = -C_M[i](D_i/RT)(Q_i^* \,\delta \ln T/\delta x + (\delta \eta_i/\delta x)_T) \quad (10)$$

where Q_i^* is the heat of transport and $d\eta_i = d\mu_i = RT\, d \ln a_i$ in the considered material (eqn (7)).

In the following, the two driving forces which appear in eqn (10) will be considered successively and consequently the mean mechanisms leading to a cation flow and to a demixing process of the species, under a temperature gradient.

2.3.1 Thermal driving force ($\nabla \ln T$)

It can be recalled that the diffusion coefficient of a cationic species i by a vacancy mechanism depends on the probability of finding a vacancy near the cation. It is then proportional to the molar concentration of vacancies and can be written as follows:

$$D_i = \beta a^2 f_i \omega_i [V^{\alpha'}] \quad (11)$$

where β is a geometrical factor that only depends on the crystal structure $[V^{\alpha'}]$, the mole fraction of cationic vacancies ionized α-times, a the elementary jump length, f_i a correlation factor that takes into account the non-random motion of the cationic species induced by the vacancies and ω_i the exchange frequency between a vacancy and a surrounding cation. It may be noted that the product $f_i\omega_i$ is often called the effective jump frequency between a vacancy and a surrounding cation (i.e. jumps which are effective for a macroscopic displacement). It can be recalled that in an oxide solid solution (A, B)O the average effective exchange frequency of a vacancy can be calculated as the weighted average of the effective exchange frequencies ($f_A\omega_A$ and $f_B\omega_B$) of the cations:[17-19]

$$f\omega = [AO]f_A\omega_A + [BO]f_B\omega_B$$

(where [AO] and [BO] are the mole fractions of the oxides AO and BO in the solid solution, respectively).

The thermal driving force is due to the thermally activated process of the exchange frequency (ω_i) between the vacancy and a surrounding cation. Indeed, ω_i is proportional to the probability for the cation to jump in a vacancy site and can be written:

$$\omega_i = \nu_i \exp -\Delta G_m/RT \quad (12)$$

where, ν_i is the vibrational frequency of the cation in the direction of the vacancy and ΔG_m ($=\Delta H_m - T\Delta S_m$) the activation free energy of migration (which corresponds to the height of the saddle point).

The effect of temperature on atomic diffusion appears through the enthalpy of migration, ΔH_m. The jump frequency of a cation in a vacancy is then higher for the cations in the higher temperature side ($\delta\omega_i/\delta T > 0$) and for those with a lower enthalpy of migration. The difference of temperature then has the effect of causing the cations to move from the higher to the lower temperature side. Furthermore, these transport processes can lead to a kinetic demixing of the cations A and B if their heats of transport (Q_i^*) are different. (In a simple vacancy mechanism as considered previously, ΔH_m is the magnitude of the heat of transport. In a macroscopic point of view the hopping of a cation in a vacancy generally involves the cooperative motion of several atoms. Furthermore, other mechanisms can also be considered. Nevertheless, few data have been available in the literature until now. After Yoo & Wuensch[20] it seems that the magnitude of the heat of transport (Q_i^*) involved in such processes is at most the enthalpy of migration ($Q_i^* \leq \Delta H_m$).)

2.3.2 Chemical driving force ($\nabla \mu_i$)

As shown in the following this driving force can be identified with the vacancy concentration gradient which can set up in the material under a temperature gradient. This driving force is then equivalent to that which appears in the material under an oxygen

potential gradient at constant temperature (eqns (4), (8) and (9)).

Consider an oxide (A, B)O in the form of a plate of thickness x whose main surfaces are exposed to different temperatures, at constant P_{O_2}. According to the local thermodynamical equilibrium condition (eqns (1)–(3)), a lower concentration of vacancies then appears on the side exposed to the lower temperatures, if $\Delta H_f > 0$, or on the opposite side, if $\Delta H_f < 0$. This leads to a vacancy concentration gradient which is given in the present case (eqns (2) and (3)) by the following expression:

$$(\delta \ln [V^{x'}]/\delta x)_{P_{O_2}} = \frac{\Delta H_f}{(1+\alpha)RT} \frac{\delta \ln T}{\delta x} \qquad (13)$$

This vacancy concentration gradient leads to a flux of vacancies in the direction of the lower concentration of vacancies, i.e. toward the side of the lower temperatures, if $\Delta H_f > 0$, or in the opposite direction, if $\Delta H_f < 0$. This flux of vacancies is of course accompanied by a flux of cations in the opposite direction. Far from vacancy sources and sinks lattice sites are conserved and these fluxes are coupled according to eqn (5).

Due to the chemical driving force a kinetic demixing takes place in the material if the diffusivities (eqn (11)) of the cations A and B are different ($D_A \neq D_B$).[16] Indeed, the exchange frequency between a vacancy and a surrounding cation (eqn (12)) is lower for the less mobile cations. If the correlation effects between the jumps of the cations A and B can be neglected (the off-diagonal elements L_{ij} in a phenomenological formulation), an enrichment of the less mobile cations occurs near the side corresponding to the lower vacancy concentrations, i.e. near the side exposed to the lower temperatures, if $\Delta H_f > 0$, or on the opposite side, if $\Delta H_f < 0$. (It may be noted that the transport processes due to the thermal driving force and those due to the chemical driving force are in the same direction when $\Delta H_f < 0$, and in the opposite direction if $\Delta H_f > 0$.)

2.4 Relative magnitude of the two driving forces

Experiments reported by Petuskey & Bowen[3] have allowed them to detect the vacancy flow which appears in an iron aluminate spinel exposed to a temperature gradient under different boundary conditions. In a first experiment the exchanges between the specimen and the surrounding atmosphere were possible. At the end of the experiment, they observed an enrichment of aluminum near the side exposed to the higher temperature and a displacement of platinum markers attached to the end of the sample exposed to the lower temperature. This set of results confirms a net vacancy flow toward the higher temperature side (the enthalpy of formation of the defects is then negative—$\Delta H_f < 0$). Because of the greater diffusivity of iron ($D_{Fe} > D_{Al}$, cf. Ref. 3) it migrates more rapidly than aluminium and therefore enriches the colder regions, whereas an enrichment of aluminium occurs in the hotter regions. In a second experiment, the sample was encapsulated in a platinum foil. The exchange with the surrounding atmosphere was not possible and the sample was exposed only to the thermal driving force. At the end of the experiment the enrichment of aluminium near the higher temperature side was negligible and no evident movement of the markers was observed. It follows from this experiment that the matter transport due to the thermal driving force is negligible. Consequently, the cation demixing effect observed in the first experiment seems to be caused primarely by the mass transport related to the driving force of the vacancy concentration gradient created by the temperature gradient (eqn (13)). This conclusion has been confirmed by calculations done by Ishikawa *et al.*[5] in a closed system.

According to this set of data, in the following the transport processes due to the thermal force field have been neglected. With this approximation, eqn (10) becomes:

$$J_i = -C_M[i](D_i/RT)(\delta \mu_i/\delta x)_T \qquad (14)$$

where $(\delta \mu_i/\delta x)_T$ is the chemical potential gradient of the component i (i.e. of the neutral species) due to the vacancy concentration gradient which appears under a temperature gradient, at constant P_{O_2} (eqn (13)).

Therefore, using the same assumptions as previously (cf. Section 2.2) under an oxygen potential gradient (local chemical equilibrium between the different species in each element of volume during the transport processes, electroneutrality condition), it has been shown that eqns (8) and (9) can be applied to the transport processes under a temperature gradient, at constant P_{O_2}:

$$J_{A^{2+}} = C_M D_A(\delta m/\delta x + (1-m)(1+\alpha)\,\delta \ln [V^{x'}]/\delta x) \qquad (15)$$

$$J_{B^{2+}} = C_M D_B(-\delta m/\delta x + m\gamma(1+\alpha)\,\delta \ln [V^{x'}]/\delta x) \qquad (16)$$

but in these last equations the vacancy concentration gradient $\delta \ln [V^{x'}]/\delta x$ is given by eqn (13).

Equations (15) and (16) allow the problem of cation redistributions under a temperature gradient to be reduced to a problem of diffusion under a vacancy concentration gradient. Therefore, the

present problem can be treated as previously[10] when the sample is exposed to a chemical potential gradient at constant temperature (eqns (8) and (9)) but with the boundary condition that the concentration of vacancies on the end surfaces of the sample is fixed by T instead of P_{O_2}. In the calculations it has been taken into account that the diffusion coefficients are function of temperature. This has allowed the estimation of the time-dependent concentration profile of cations ($m = f(x, t)$) in (Co, Mg)O oxide solid solutions subjected to temperature gradients.

3 Time Evolution of Concentration Profiles

Calculations are done for simplicity in the crystal reference frame. Consequently, in the following a distinction is made between the crystal reference frame, which coincides with the end surfaces of the sample, and the laboratory reference frame, which coincides with the immobile oxygen sublattice. This has allowed the shift velocity of the end surfaces of the sample with respect to the laboratory reference frame to be considered first.

3.1 Shift velocity of the end surfaces and boundary condition

As has been shown previously all the transport processes under thermodynamic potential gradients occur through the immobile oxygen sublattice. Consequently, it is easier to describe the flux of mobile species with respect to this reference frame as has been done until now (eqns (8), (9), (13) and (14)). Nevertheless, during the transport processes a simultaneous destruction and formation of the two sublattices occur at the low and at the high vacancy concentration sides. According to eqn (1), this leads to a shift of the end surfaces in the direction of the higher vacancy concentration side. Cation redistributions then occur in the sample, while it moves with respect to the laboratory reference frame. Consequently, in order to be able to simulate the segregation profiles of the mobile species it is meaningful to express their fluxes with respect to the end surfaces of the sample.

3.1.1 Calculation assumption

Calculations have been done assuming that the two end surfaces move with the same velocity (i.e. the length of the sample remains constant during the transport processes). With this approximation the simulated results of kinetic demixing will correspond to time (Δt^v) higher than those needed for vacancies to percolate through the entire length of the specimen, i.e. to reach the steady-state condition (if the small vacancy concentration changes due to the redistribution of cations are neglected).

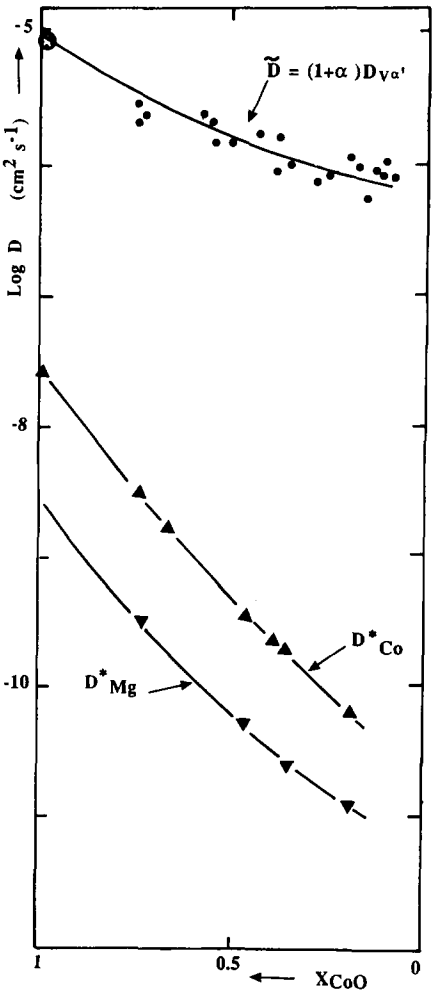

Fig. 2. Diffusion coefficients of Co (D^*_{Co}) and Mg (D^*_{Mg}) as a function of the composition in (Co, Mg)O solid solutions. Comparison with the chemical diffusion coefficient ($\tilde{D}$) whose values are close to the diffusion coefficient of the vacancies (eqn (17)). $P_{O_2} = 0{\cdot}2$ bar; $T = 1573$ K.

$$D_i^* = D_i^{*0} \exp(-E_i/RT) \exp(b_i x + c_i x^2)\ \mathrm{cm^2\ s^{-1}}$$

with[21]

$$D^{*0}_{Co} = 1{\cdot}12 \times 10^{-5} \qquad E_{Co} = 172\,400\ \mathrm{J\ mol^{-1}}$$
$$b_{Co} = 5{\cdot}54 \qquad c_{Co} = 1{\cdot}67$$
$$D^{*0}_{Mg} = 3{\cdot}61 \times 10^{-6} \qquad E_{Mg} = 174\,600\ \mathrm{J\ mol^{-1}}$$
$$b_{Mg} = 3{\cdot}32 \qquad c_{Mg} = 2{\cdot}88$$

$$\tilde{D}_{(\mathrm{pure\ CoO})}{}^{22} = 0{\cdot}13 \exp(125\,400\ \mathrm{J\ mol^{-1}})/RT\ \mathrm{cm^2\ s^{-1}}$$

●, Schwier *et al.*[23] ——, calculated[21] with D^*_{Co}, D^*_{Mg} and x_V; ✪ Petot-Ervas *et al.*;[22] ▲ and ▼, Schnehage *et al.*[21]

Because of the differences in the magnitude of the diffusion coefficient for vacancies and cations ($D_{V^{z'}} \gg D_i$), the time Δt^v corresponds to the very early stage of the transient period as will be seen in the following. Indeed, as an example, in Fig. 2 the diffusion coefficient of Co and Mg is reported as a

function of the composition of the (Co, Mg)O solid solution as well as the chemical diffusion coefficient ($\tilde{D}$), whose values are close to the diffusion coefficient of the vacancies ($D_{V^{\alpha'}}$). Indeed, $\tilde{D}$ can be written as follows:[13]

$$\tilde{D} \simeq (1+\alpha)D_{V^{\alpha'}} \tag{17}$$

According to this set of data the time Δt^{v} has been estimated from the time needed for the vacancy to percolate through the material ($L \simeq \sqrt{\Delta t^{v} . D_{V^{\alpha'}}}$, where L is the length of the specimen). Δt^{v} was found to be lower than 0·5 h for the kinetic demixing results given in Fig. 1 and obtained with (Co, Mg)O samples of 1 mm length. This estimation is in agreement with the numerical solution[10] which shows that the vacancy concentration gradient reached a quasi-steady-state profile after about 0·5 h with small deviations (lower than 0·2%), due to the cation demixing effects on the vacancy concentration. It may be noted that no noticeable changes in cation concentrations were observed during this lapse of time.

3.1.2 Shift velocity of the end surfaces

It can be pointed out that the cationic sublattice grows on the high vacancy concentration side not only with the arrival of cations ($\Delta N_C = J_A + J_B$, per unit surface area and time) but also with the formation of cationic vacancies in thermodynamical equilibrium with the surrounding atmosphere and formed according to eqn (1) ($\Delta N_V = ([V^{\alpha'}]/([A]+[B]) . \Delta N_C$). Consequently, the total number of cationic sites which are formed, per unit surface area and time, can be expressed as:

$$\Delta N_C + \Delta N_V = (J_A + J_B)\left(1 + \frac{[V^{\alpha'}]}{[A]+[B]}\right) \tag{18}$$

The same equation holds at the opposite side, where cationic sites are destroyed. Consequently, if a sample is considered in the form of a plate of thickness L whose main surfaces are exposed to different temperatures, this leads to a displacement of the opposite surfaces (per unit time) of a length $\Delta x = (\Delta N_C + \Delta N_V)/C_M$. This length is then equal to the shift velocity of the end surfaces of the sample with respect to the laboratory reference frame when the steady state (or the quasi-steady state) is reached for the vacancies. This yelds:

$$v = \frac{J_A + J_B}{C_M(1-[V^{\alpha'}])} = \frac{-J_V}{C_M(1-[V^{\alpha'}])} \tag{19}$$

The concentration of vacancies being generally small in the considered materials ($[V^{\alpha'}] \ll 1$), it is possible to neglect their concentration. With this assumption, the drift velocity of the end surfaces of the sample, with respect to the laboratory reference frame, can be written:

$$v \simeq (J_A + J_B)/C_M = -J_V/C_M \tag{20}$$

3.1.3 Boundary condition

On the end surfaces of the sample (if there is no evaporation) it has to be taken into account that the shift velocity of the cations A and B is equal to the shift velocity of these surfaces ($v = v_A = v_B$) with respect to the laboratory reference frame. Thus the following relation between the different fluxes is obtained:

$$-J_V/C_M = J_A/(1-m)C_M = J_B/mC_M \tag{21}$$

According to eqns (15) and (16), this leads to a boundary condition between the concentration gradient of vacancies and cations close to the surfaces of the sample:

$$\delta m/\delta x = \frac{m(1-m)(\gamma D_B - D_A)}{(1-m)D_B + mD_A}(1+\alpha)\,\delta \ln [V^{\alpha'}]/\delta x \tag{22}$$

It may be noted that this boundary condition implies that the distribution of vacancies is established quickly compared to the cation distribution changes. This assumption is consistent with the relative diffusion coefficient values of vacancies and cations (cf. Fig. 2, for instance). Indeed, as for the pure oxides (where $D_i = [V^{\alpha'}]D_{V^{\alpha'}}$), it can be considered with a good approximation that in solid solutions the ratio of the relaxation times for cations and for vacancies (eqns (11) and (17)) is close to the molar vacancy concentration, i.e. generally smaller than 10^{-2}.

3.1.4 Steady-state condition for the cations[6-10]

The kinetic demixing profile of the cations at the steady state remains constant while the crystal moves with a constant velocity (with respect to the laboratory reference frame). Consequently, all the species move with the same velocity in the crystal (eqn (21)) and the condition expressed by eqn (22) is then reached in all of the sample.

3.2 Change of reference frame

In the following the prime denotes the fluxes with respect to the moving reference frame. Consequently, it follows from eqn (19) that the transformation equations between the two reference frames considered can be written as follows:

$$J'_A = J_A + J_V(1-m-[V^{\alpha'}])/(1-[V^{\alpha'}]) \tag{23a}$$

$$J'_B = J_B + J_V m/(1-[V^{\alpha'}]) \tag{23b}$$

$$J'_V = J_V + J_V[V^{\alpha'}]/(1-[V^{\alpha'}]) \tag{24}$$

and the corresponding equation of conservation of lattice sites (far from vacancy sources and sinks) if $[V^{\alpha'}] \ll 1$ is given as:

$$J'_A + J'_B = 0 \tag{25}$$

Substituting eqns (15) and (16) into eqns (23)–(25) yields:

$$J'_B/C_M = -J'_A/C_M = ((m-1)D_B - mD_A)\,\delta m/\delta x + m(1-m)(\gamma' D_B - D_A)(1+\alpha)\,\delta \ln [V^{\alpha'}]/\delta x \tag{26}$$

$$J'_V/C_M = (D_B - D_A)\,\delta m/\delta x - (m\gamma' D_B + (1-m)D_A)(1+\alpha)\,\delta \ln [V^{\alpha'}]/\delta x \tag{27}$$

The transport processes under a gradient of temperature can be described, in the crystal reference frame, by the two last equations. Therefore, an analytical solution of the kinetic demixing profiles can be obtained by solving these equations as a function of time. If diffusion occurs in the x-direction, one can write for the species i (where i can be B and V) according to the conservation laws:

$$d[i]/dt = -div(J'_i/C_M) \tag{28}$$

(It may be noted that heat conduction is generally much more rapid than mass transport even in refractory materials. Consequently, when the sample is exposed to a temperature gradient it has been assumed that a linear steady-state temperature distribution ($\delta T/\delta x = \text{constant}$) is reached within a time negligibly small compared to that which leads to measurable changes in concentration.)

3.3 Numerical solution—kinetic demixing in a (Co, Mg)O sample, and discussion

There are few systems in the literature with sufficient information concerning the transport and physical properties to allow the extent of demixing that can be expected under a temperature gradient to be calculated. Consequently, in order to illustrate the rate at which the dehomogenization occurs calculations have been done for the (Co, Mg)O solid solutions which have been widely studied by Schmalzried and coworkers.[17,21,23]

According to eqns (26) and (27) the time-dependent differential equation (eqn (28)) has been solved using the finite difference technique.[24] To calculate the composition at any point during the transient period, and until a steady state has been reached, it has been assumed that the concentration of vacancies on the end surfaces of the sample are established quickly after a change of temperature. Consequently, after a fast transient process has taken place, the vacancy concentrations on the sample surfaces are given by the condition of the local thermodynamical equilibrium (eqns (2) and (3)). For calculation the origin of the coordinate has been taken on one side of the sample whose length is L. If $[V^{\alpha'}]^0$ and $[V^{\alpha'}]^L$ are the vacancy concentrations on the end surfaces (fixed by the temperature—eqn (2)), this leads to the following boundary conditions on the end surfaces:

$$[V^{\alpha'}](x=0,t) = [V^{\alpha'}]^0 \tag{29}$$

$$[V^{\alpha'}](x=L,t) = [V^{\alpha'}]^L \tag{30}$$

with the initial condition of an homogeneous concentration of vacancies and cations (flat profile):

$$[V^{\alpha'}](x,t=0) = [V^{\alpha'}]^0 \tag{31}$$

$$m(x,t=0) = m_0 \tag{32}$$

Furthermore, it has been assumed that the cations are conserved in the oxide (no evaporation on the end surfaces). This condition corresponds to eqn (21) and can be written, for the cations B for example, as follows:

$$J'_B(x=0,t) = J'_B(x=L,t) = 0 \tag{33}$$

3.3.1 Kinetic demixing in the (Co, Mg)O solid solutions

A complete set of thermodynamic and kinetic results are available for the (Co, Mg)O solid solution. Nevertheless, the authors have made in a first approach some assumptions in order to reduce the time of calculation.

It can be recalled that the semi-conducting oxides CoO and MgO form an almost ideal complete solid solution in which the prevailing defects are cationic vacancies neutralized by electron holes (eqn (1)). Schmalzried and coworkers[17,21,23] have determined the concentration of cationic vacancies and their mean charge as a function of temperature and composition as well as the Co and Mg diffusion coefficient values (Fig. 2). They have shown that it is a good approximation to consider that the vacancy concentration is an exponential function of the mole fraction of MgO. Furthermore, they have observed that the mean charge of the vacancies (α) depends on composition and varies from $\alpha = 1$ for CoO-rich solid solutions to $\alpha = 2$ when the solid solutions are rich in MgO.

In a first approximation it has been assumed that the mean charge of the vacancies does not change during the transport process and equals the value corresponding to the initial composition and temperature (for a sample with an initial concentration $m = 0{\cdot}49$ at $T = 1773$ K, $\alpha = 1{\cdot}7$).

In a second approximation, it has been assumed that the concentration of vacancies on the end

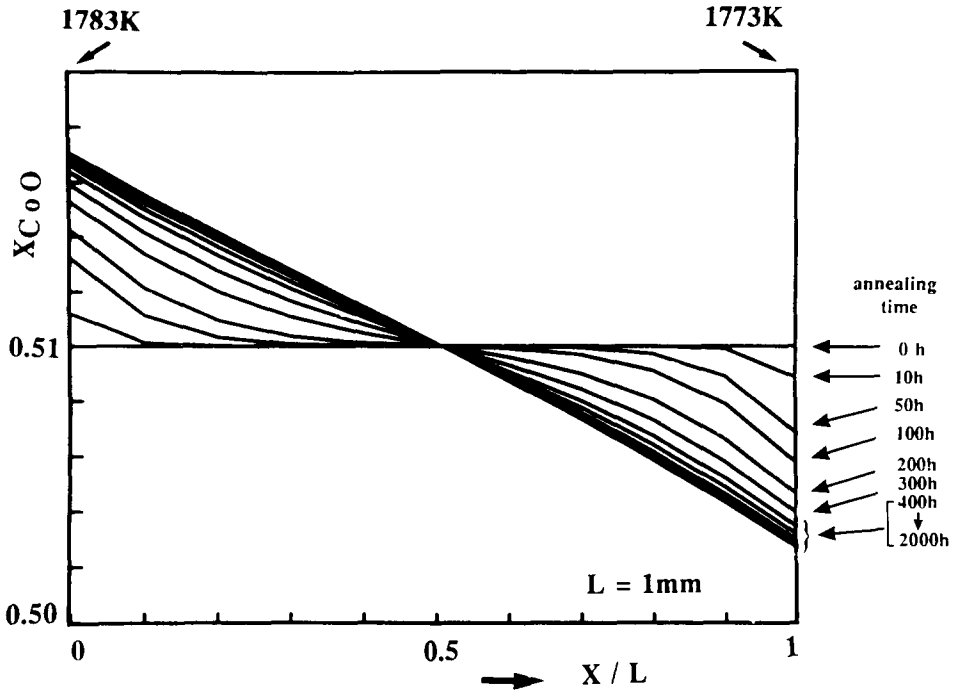

Fig. 3. Time evolution of the kinetic demixing in a (Co, Mg)O sample of 1 mm length annealed in a temperature gradient between 1773 and 1783 K at $P_{O_2} = 0{\cdot}21$ atm. (The segregation profiles for MgO can be calculated according to the relation between the molar fraction: $x_{MgO} = 1 - x_{CoO}$.) (The numerical solution was obtained by introducing dimensionless variables of position x/L (L is the total length of the sample and x the coordinate in the crystal reference frame). A grid was defined with a time interval $\delta t = 3{\cdot}8$ s and a space interval of $\delta L = 0{\cdot}1$ mm.)

surfaces do not vary with the development of the demixing.

As an example, in Fig. 3 the time evolution of the kinetic demixing calculated for a (Co, Mg)O sample with an initial magnesium mole fraction $m = 0{\cdot}49$ is reported. This sample, of 1 mm length, has been assumed exposed in air under a temperature gradient between 1773 and 1783 K. It follows from these simulations that it takes more than 600 h to reach a steady state. The results reported in Fig. 4 shows the influence of the mean temperature on the cation redistributions at a given time ($t = 570$ h) while those reported in Fig. 5 indicate the effect of the temperature gradient on the magnitude of the composition difference across the sample. The values of the concentration profile of CoO calculated for two samples of different length (1 mm and 10 mm) and exposed under the same temperature gradient ($10\ mm^{-1}$) are compared in Figs 6 and 7. As expected, the kinetic demixing effects are most easily observed across the sample when its thickness decreases (Fig. 6) because the transport distance is smaller. Nevertheless, it is important to note (Fig. 7) that the segregation effects are more pronounced near the surface when the length of the sample increases. As will be seen in the discussion this unexpected result near the surface is consistent with the fact that the times needed to reach either a quasi-steady state for the vacancies (Δt^{v}—time needed for

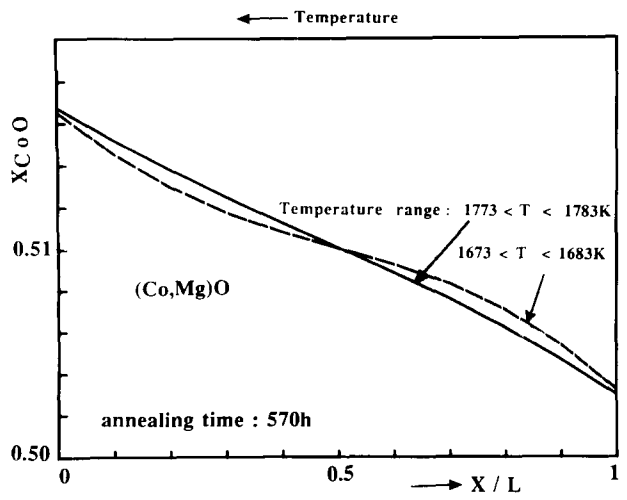

Fig. 4. Influence of the temperature range on the segregation profiles of CoO in a (Co, Mg)O sample of 1 mm length annealed under the same temperature gradient but in two different ranges ($1\,683\,K > T > 1673\,K$ and $1783\,K > T > 1773\,K$ for 570 h. (The same cation segregation profiles will be reached at the steady state, but in a shorter time in the higher temperature range.)

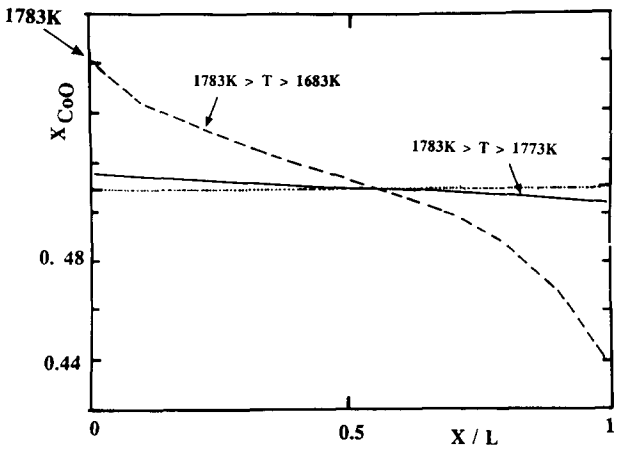

Fig. 5. Influence of the temperature gradient on the segregation profiles of CoO in a (Co, Mg)O sample of 1 mm length annealed under two different temperature ranges ($1783\,K > T > 1773\,K$ and $1783\,K > T > 1683\,K$ for 400 h.

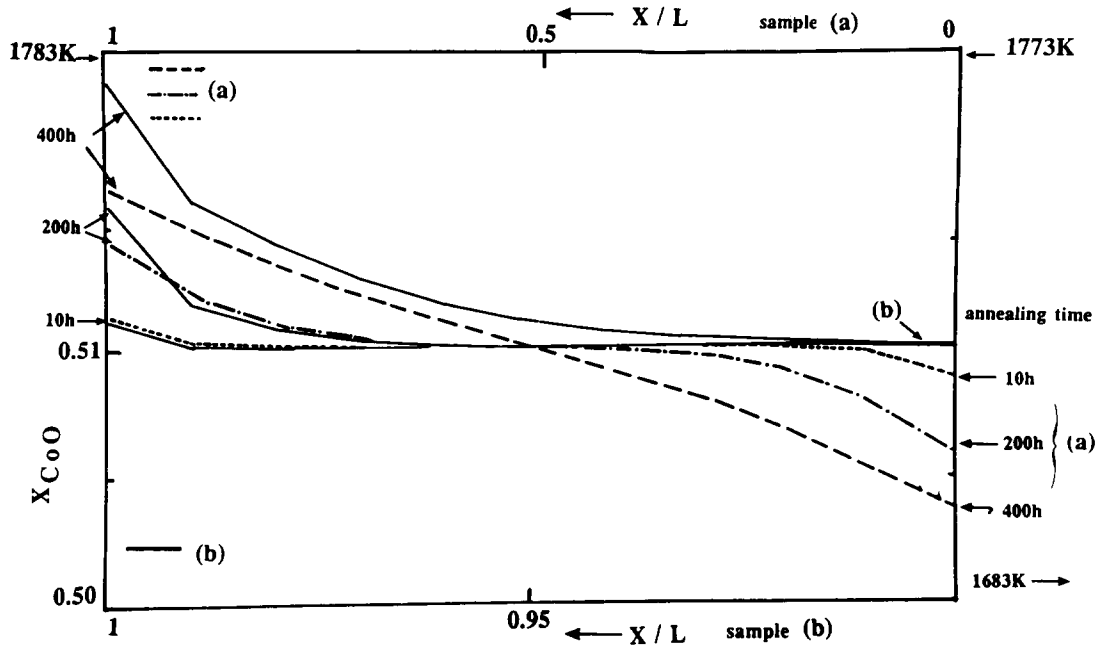

Fig. 6. Comparison of the calculated segregation profiles of CoO across two (Co, Mg)O samples of (a) 1 mm and (b) 10 mm length, respectively, and annealed under the same temperature gradient ($\delta T/\delta x = 10^{\circ}\,\mathrm{mm}^{-1}$). Temperature ranges: (a) 1783 K > T > 1773 K; (b) 1783 K > T > 1683 K.

a vacancy to percolate through the entire length of the specimen) or a constant cation concentration profiles (Δt^{s}—time needed to reach the steady state[6-10]—cf. Section 3.1.4) increase with the sample thickness. These times are roughly proportional to the square of the length ratio:

$$\Delta t_2 \simeq (L_2/L_1)^2\,\Delta t_1 \qquad (34)$$

where L_1 and L_2 are the length of the samples (with $L_2 > L_1$), Δt_1 and Δt_2 are the times needed to reach either a quasi-steady state for the vacancies (Δt^{v}) or a steady state for the cations (Δt^{s}) in sample 1 (length L_1) and in sample 2 (length L_2), respectively.

3.3.2 Discussion

To explain the unexpected increase of the kinetic demixing near the surfaces when the length of the sample increases it is necessary to consider the different mean steps during the transient period.

The first step corresponds to the transport

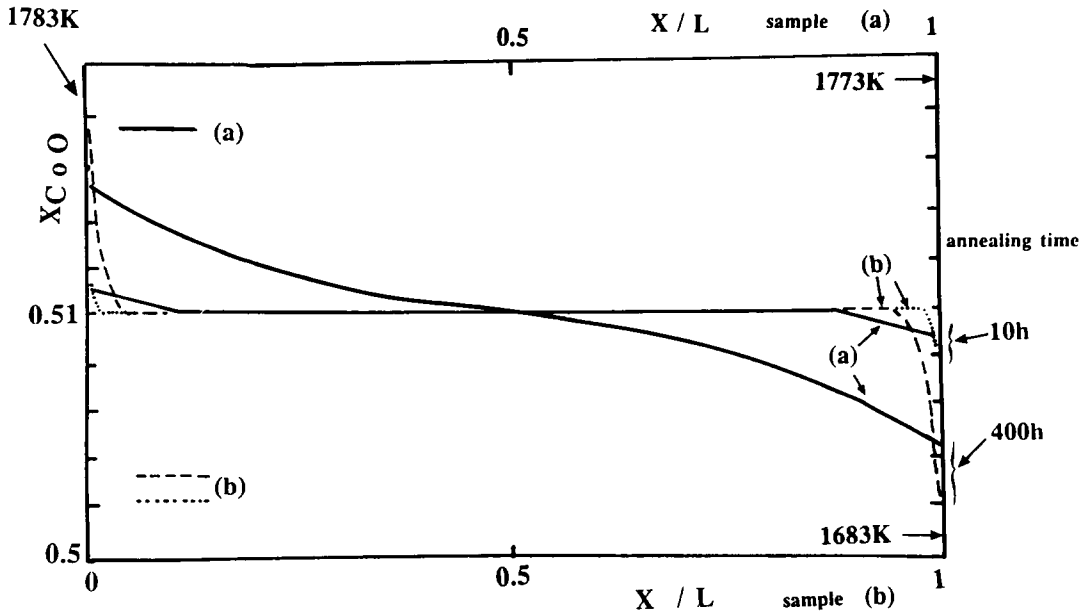

Fig. 7. Comparison of the segregation profiles of CoO calculated over 1 mm depth for two (Co, Mg)O samples of (a) 1 mm and (b) 10 mm length, respectively, and annealed under the same temperature gradient ($\delta T/\delta x = 10^{\circ}\,\mathrm{mm}^{-1}$). Temperature ranges: (a) 1783 K > T > 1773 K; (b) 1783 K > T > 1683 K.

processes which occur during the time needed for the vacancies to reach the quasi-steady state ($0 < t < \Delta t^{v}$), i.e. during the very early stage of the transient period (cf. Section 3.1.1). According to eqn (34), the time Δt^{v} is directly related to the sample length and it has been found lower than 0·5 h for a sample of 1 mm length, for example (cf. Section 3.1.1). During this step, the vacancy concentration profile at any time is given by an error function [24] (solution of eqn (28) with $J_V = -C_M D_V(\delta[V^{x'}]/\delta x)$ and with the boundary condition of a constant concentration of vacancies on the sample surface. Indeed, after an abrupt change of the thermodynamic equilibrium conditions the concentration of vacancies on the surface is given by eqn (2) (local equilibrium condition). This leads to a sharp concentration gradient of vacancies ($\delta \ln [V^{x'}]/\mathrm{d}x$) near the surfaces, which then develops in the sample until the quasi-steady state has been reached. (For an identical temperature gradient through the sample, the abrupt change of the concentration of vacancies is higher for the largest sample. Consequently, from the start of the perturbation the flux of vacancies will be higher in the largest sample.)

Simultaneously to the development of the vacancy concentration gradient, cation redistributions occur near the surfaces. Nevertheless, calculations show that the cation redistributions during this step ($t < \Delta t_1^{v}$) do not lead to noticeable changes in cation concentrations through the sample ($\delta m/\delta x \simeq 0$). Consequently, according to eqn (27), the vacancy flux in the sample is then given to a good approximation by the following equation:

$$J_V/C_M = -(m_i' D_B + (1-m) D_A)(1+\alpha)\,\delta \ln [V^{x'}]/\delta x$$
$$= -A\,\delta \ln [V^{x'}]/\delta x \qquad (35)$$

which shows that during this step the vacancy flux varies in the crystal and this variation is directly related to the development of the vacancy concentration gradient through the sample.

The second step: when $t \geq \Delta t_1^{v}$, a quasi-steady state is reached for the vacancies in sample 1 ($\delta \ln [V^{x'}]/\delta x = \mathrm{cst}$). Therefore, the cation concentration gradients corresponding to the steady state condition (eqn (22)) start to develop from the surfaces toward the bulk of crystal. (It may be noted that the condition given by eqn (22) is reached for the cations in all the sample at the steady state—cf. Section 3.1.4). If eqn (27) is written as follows:

$$J_V/C_M = (D_B - D_A)\,\delta m/\delta x - A\,\delta \ln [V^{x'}]/\delta x \qquad (36)$$

the first term in eqn (36) soon cannot be neglected. This equation shows that the flux of vacancies then decreases when the kinetic demixing ($\delta m/\delta x$) increases through the sample. Indeed, the first and second term ($A > 0$) in the expression of J_V have opposite signs whatever the relative values of D_A and D_B. Such variations are confirmed by the simulated results reported in Fig. 8. It may be noted that J_V decreases through the sample until the steady state for the cations has been reached (eqn 22)—cf. Section 3.1.4).

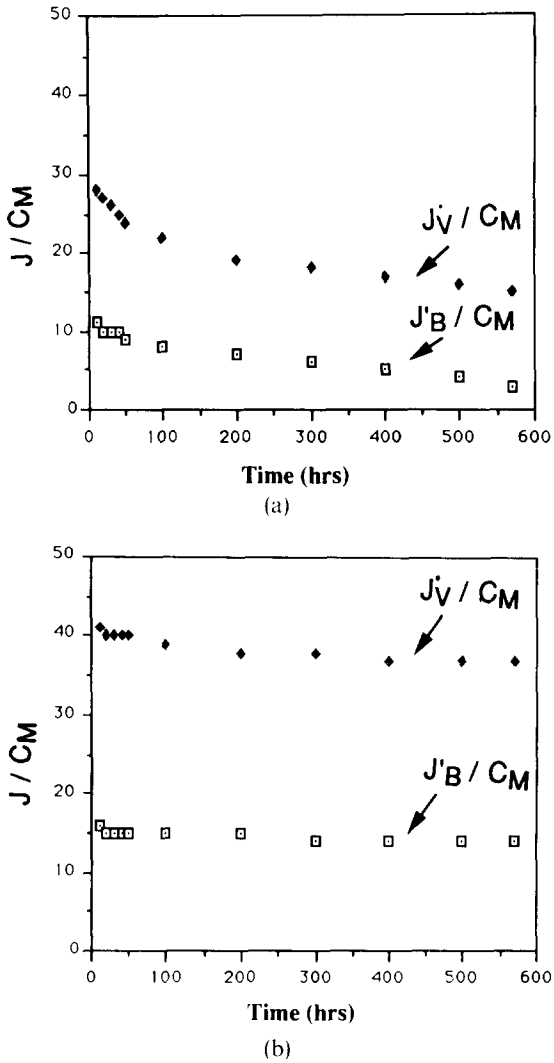

Fig. 8. Vacancy fluxes as a function of time in the middle of two samples of (a) 1 mm and (b) 10 mm length, respectively, and annealed under the same temperature gradient ($\delta T/\delta x = 10\ \mathrm{mm}^{-1}$). Temperature ranges: (a) 1783 K > T > 1773 K; (b) 1783 K > T > 1673 K.

Whereas the smallest sample (crystal 1) has reached the second step ($t > \Delta t_1^{v}$) the largest sample (crystal 2) is still at the first step until $t = \Delta t_2^{v}$. Consequently, when $t > \Delta t_2^{v}$, the vacancy flux decreases from a longer time in crystal 1 (which reaches the minimum value before the larger one—$\Delta t_1^{s} < \Delta t_2^{s}$) than in crystal 2, at a given time. The vacancy flux then stays high for a longer time in the largest sample. It may be noted that this analysis is confirmed by the results reported in Fig. 8, which

shows that the vacancy flux in the middle of the largest sample is higher than that in the middle of the smallest. Consequently, according to the boundary condition given by eqn (21), the cationic fluxes near the surfaces of the largest sample must be higher than those in crystal 1. The cation redistributions, being directly related to the cationic fluxes, lead to a higher kinetic demixing near the surface of the largest sample, as observed in Fig. 7.

The experimental work is in progress in order to check the results of these calculations. Nevertheless, it can be pointed out that the main assumptions of this treatment have been confirmed previously[10] when calculations have been done for (Co, Mg)O samples exposed under a chemical potential gradient at constant temperature.

4 Conclusion

In this study the authors have treated the transport processes under a temperature gradient as a problem of diffusion under a vacancy concentration gradient. The diffusion equations as a function of time have been solved by a numerical method under appropriate simplifying conditions and assuming that the quasi-steady state for the vacancies has been reached. This has allowed the prediction of how demixing evolves with time. The calculation has been applied to (Co, Mg)O solid solutions for which thermodynamic and transport properties are available. The predicted cation redistributions show that the magnitude of these kinetic demixing effects are far from negligible even for small temperature gradients. The composition changes can be particularly important near the surfaces which are the sources and sinks of the defects responsible for the matter transport. Since ceramics are used quite often in high-temperature environments, these effects are then an important source of deterioration. Consequently, such studies will, in future, provide an evaluation and consequently a guarantee of the service performance of these materials in high-temperature environments.

References

1. Petot-Ervas, G. & Petot, C., Surface segregation in ceramic materials during cooling or under a temperature gradient. *J. Eur. Ceram. Soc.*, **6** (1989) 323–30.
2. Petot-Ervas, G., Dynamic segregation in multicomponent oxides under chemical potential gradients. In *Surfaces and Interfaces of Ceramic Materials*, ed. L. C. Dufour, C. Monty & G. Petot-Ervas. Kluwer Academic Press, Vol. 173, 1989, pp. 337–49.
3. Petuskey, W. T. & Bowen, H. K., Thermal segregation of cations in iron aluminate spinels. *J. Am. Ceram. Soc.*, **64** (1981) 611–16.
4. Akbar, S. A., Kaburagi, M., Sato, H. & Kikuchi, R., Demixing of oxides under a temperature gradient. *J. Am. Ceram. Soc.*, **70** (1988) 246–53.
5. Ishikawa, T., Sato, H., Kikuchi, K. & Akbar, S. A., Demixing of materials under chemical potential gradients. *J. Am. Ceram. Soc.*, **68** (1985) 1–6.
6. Schmalzried, H., Behavior of oxide crystals in oxygen potential gradients. *Reactivity of Solids*, **1**, (1985) 117–37.
7. Schmalzried, H., Laqua, W. & Lin, P. L., Crystalline oxide solid solutions in oxygen potential gradients. *Z. Naturforsch.*, **34a** (1979) 192–99.
8. Schmalzried, H. & Laqua, W., Multicomponent oxides in oxygen potential gradients. *Oxidation of Metals*, **15** (1981) 339–53.
9. Petot-Ervas, G. & Petot, C., The influence of impurities segregation phenomena on the oxido-reduction kinetics of oxides. *J. Phys. Chem. Solids*, **51** (1990) 901–6.
10. Monceau, D., Petot, C. & Petot-Ervas, G., Segregation profile calculation in oxide solid solutions under a chemical potential gradient. *Solid State Ionics*, **45** (1991) 231–7.
11. Wolfenstite, J., Dimos, D. & Kohlstedt, D., Decomposition of Ni_2SiO_4 in an oxygen potential gradient. *J. Am. Ceram. Soc.*, **68** (1985) C117–C118.
12. Ishikawa, T., Akbar, S. A., Zhu, W. & Sato, H., Time evolution of demixing in oxides under an oxygen potential gradient. *J. Am. Ceram. Soc.*, **71** (1988) 513–20.
13. Kofstad, P., *Nonstoichiometry, Diffusion and Electrical Conductivity in Binary Metal Oxides*. J. Wiley, Interscience, New York, 1972.
14. Wagner, C., The distribution of cations in metal oxide and metal sulphide solid solutions formed during the oxidation of alloys. In *Corrosion Science*, Vol. 9. Pergamon Press, 1969, pp. 91–109.
15. Howard, R. E. & Lidiard, A. B., Matter transport in solids. *Rep. Progress in Physics*, **27** (1964) 161–240.
16. Gillan, M. J., Diffusion in a temperature gradient. In *Mass Transport in Solids*, Vol. 97, ed. F. Benière & C. R. A. Catlow. Plenum Press, New York, 1982, pp. 227–50.
17. Dieckmann, R. & Schmalzried, H., Point defects in oxide solid solutions, *Ber. Bunsenges. Phys. Chem.*, **79** (1975) 1108–14.
18. Philibert, J., *Diffusion in Solids*. Les Editions de Physique, Paris, 1987.
19. Manning, J. R., *Diffusion Kinetics for Atoms in Crystals*. D. Van Nostrand Comp. Inc., Princeton, 1968.
20. Yoo, H. I. & Wuensch, B. J., Concentration distribution for diffusion in a temperature gradient. In *Transport in Nonstoichiometric Compounds*, Vol. 129, ed. G. Simkowich & V. Stubican. Plenum Press, New York, 1985, pp. 169–87.
21. Schnehage, M., Dieckmann, R. & Schmalzried, H., Point defects in oxide solid solutions (IV). Correlated diffusion of cations and vacancies in (Co, Mg)O mixed crystals. *Ber. Bunsenges. Phys. Chem.*, **58** (1982) 1061–5.
22. Petot-Ervas, G., Petot, C. & Gesmundo, F., Transport properties in p-type semiconducting oxides. *J. Phys. Chem. Solids*, **48** (1987) 767–76.
23. Schwier, G., Dieckmann, R. & Schmalzried, H., Punktfehlstellen in Oxidmischphasen. *Ber. Bunsenges. Phys. Chem.*, **77** (1973) 402–8.
24. Crank, J., *The Mathematics of Diffusion*. Clarendon Press, Oxford, 1975.